

LHC/LC Complementarity in Probing the Scalar Sector of the Randall-Sundrum Model

Jack Gunion

Davis Institute for High Energy Physics, U.C. Davis

**Collaborators: M. Battaglia, S. de Curtix, A. De Roeck, D. Dominici,
B. Grzadkowski, M. Toharia, J. Wells**

Les Houches, LHC/LC Workshop, 2003

Outline

- The parameter space
- Basics of the couplings
- Precision Electroweak Constraints
- LHC/LC Complementarity
- Conclusions

Presuming the new physics scale to be close to the TeV scale, there can be a rich new phenomenology in which Higgs and radion physics intermingle if the $\xi R \widehat{H}^\dagger \widehat{H}$ mixing term is present in \mathcal{L} .

References:

- D. Dominici, B. Grzadkowski, J. F. Gunion and M. Toharia, “The scalar sector of the Randall-Sundrum model,” arXiv:hep-ph/0206192.

- **M. Battaglia, D. Dominici, S. de Curtis, J.F. Gunion, A. de Roeck, On the Complementarity of Higgs and Radion Searches at LHC, arXiv:hep-ph/??**
- **J.F. Gunion, M. Toharia, and J. Wells, in preparation.**

Previous work:

- $\xi = 0$:

1. S. B. Bae, P. Ko, H. S. Lee and J. Lee, Phys. Lett. B 487, 299 (2000) [arXiv:hep-ph/0002224].
2. H. Davoudiasl, J. L. Hewett and T. G. Rizzo, Phys. Rev. Lett. 84, 2080 (2000) [arXiv:hep-ph/9909255].
3. K. Cheung, Phys. Rev. D 63, 056007 (2001) [arXiv:hep-ph/0009232].
4. H. Davoudiasl, J. L. Hewett and T. G. Rizzo, Phys. Rev. D 63, 075004 (2001) [arXiv:hep-ph/0006041].
5. S. C. Park, H. S. Song and J. Song, Phys. Rev. D 63, 077701 (2001) [arXiv:hep-ph/0009245].

- $\xi \neq 0$:

1. G. Giudice, R. Rattazzi, J. Wells, Nucl. Phys. B595 (2001), 250, hep-ph/0002178.
2. C. Csaki, M.L. Graesser, G.D. Kribs, Phys. Rev. D63 (2001), 065002-1, hep-th/0008151.
3. T. Han, G. D. Kribs and B. McElrath, Phys. Rev. D 64, 076003 (2001) [arXiv:hep-ph/0104074].

4. M. Chaichian, A. Datta, K. Huitu and Z. h. Yu, Phys. Lett. B 524, 161 (2002) [arXiv:hep-ph/0110035].
5. J. L. Hewett and T. G. Rizzo, hep-ph/0202155.
6. C. Csaki, M. Graesser, L. Randall and J. Terning, Phys. Rev. D 62, 045015 (2000) [arXiv:hep-ph/9911406].

Randal-Sundrum Review

Some possibly very dramatic changes in phenomenology.

- There are two branes, separated in the 5th dimension (y) and $y \rightarrow -y$ symmetry is imposed. With appropriate boundary conditions, the 5D Einstein equations \Rightarrow

$$ds^2 = e^{-2\sigma(y)} \eta_{\mu\nu} dx^\mu dx^\nu - b_0^2 dy^2, \quad (1)$$

where $\sigma(y) \sim m_0 b_0 |y|$.

- $e^{-2\sigma(y)}$ is the warp factor; scales at $y = 0$ of order M_{Pl} on the hidden brane are reduced to scales at $y = 1/2$ of order TeV on the visible brane.
- Fluctuations of $g_{\mu\nu}$ relative to $\eta_{\mu\nu}$ are the KK excitations $h_{\mu\nu}^n$.
- Fluctuations of $b(x)$ relative to b_0 define the radion field.
- In addition, we place a Higgs doublet \widehat{H} on the visible brane. After various rescalings, the properly normalized quantum fluctuation field is called h_0 .

Including the ξ mixing term

- We begin with

$$S_\xi = \xi \int d^4x \sqrt{g_{\text{vis}}} R(g_{\text{vis}}) \widehat{H}^\dagger \widehat{H}, \quad (2)$$

where $R(g_{\text{vis}})$ is the Ricci scalar for the metric induced on the visible brane.

- A crucial parameter is the ratio

$$\gamma \equiv v_0 / \Lambda_\phi. \quad (3)$$

where Λ_ϕ is vacuum expectation value of the radion field.

- After writing out the full quadratic structure of the Lagrangian, including $\xi \neq 0$ mixing, we obtain a form in which the h_0 and ϕ_0 fields for $\xi = 0$ are mixed and have complicated kinetic energy normalization.

We must diagonalize the kinetic energy and rescale to get canonical

normalization.

$$\begin{aligned} h_0 &= \left(\cos \theta - \frac{6\xi\gamma}{Z} \sin \theta \right) h + \left(\sin \theta + \frac{6\xi\gamma}{Z} \cos \theta \right) \phi \\ &\equiv dh + c\phi \end{aligned} \quad (4)$$

$$\phi_0 = -\cos \theta \frac{\phi}{Z} + \sin \theta \frac{h}{Z} \equiv a\phi + bh. \quad (5)$$

- In the above equations

$$Z^2 \equiv 1 + 6\xi\gamma^2(1 - 6\xi). \quad (6)$$

$Z^2 > 0$ is required to avoid tachyonic situation.

This \Rightarrow constraint on maximum neg. and pos. ξ values.

- The process of inversion is very critical to the phenomenology and somewhat delicate.

The result found is that the physical mass eigenstates h and ϕ cannot be too close to being degenerate in mass, depending on the precise values of ξ and γ ; extreme degeneracy is allowed only for small ξ and/or γ .

Using this inversion, for given ξ , γ , m_h and m_ϕ we compute Z^2 , $m_{h_0}^2$ and $m_{\phi_0}^2$, θ to obtain a, b, c, d in Eqs. (4) and (5).

- **Net result**

4 independent parameters to completely fix the mass diagonalization of the scalar sector when $\xi \neq 0$. These are:

$$\xi, \quad \gamma, \quad m_h, \quad m_\phi, \quad (7)$$

where we recall that $\gamma \equiv v_0/\Lambda_\phi$ with $v_0 = 246$ GeV.

Two additional parameters will be required to completely fix the phenomenology of the scalar sector, including all possible decays. These are

$$\hat{\Lambda}_W, \quad m_1, \quad (8)$$

where $\hat{\Lambda}_W$ will determine KK-graviton couplings to the h and ϕ and m_1 is the mass of the first KK graviton excitation.

There are relations among parameters:

$$\hat{\Lambda}_W \simeq \sqrt{2}M_{Pl}\Omega_0, \quad m_n = m_0x_n\Omega_0, \quad \Lambda_\phi = \sqrt{6}M_{Pl}\Omega_0 = \sqrt{3}\hat{\Lambda}_W \quad (9)$$

where $\Omega_0 M_{Pl} = e^{-m_0 b_0/2} M_{Pl}$ should be of order a TeV to solve the hierarchy problem. In Eq. (9), the x_n are the zeroes of the Bessel function J_1 ($x_1 \sim 3.8$, $x_2 \sim 7.0$). A useful relation following from the above equations is:

$$m_1 = x_1 \frac{m_0}{M_{Pl}} \frac{\Lambda_\phi}{\sqrt{6}}. \quad (10)$$

m_0/M_{Pl} is related to the curvature of the brane and should be a relatively small number for consistency of the RS scenario.

- Sample parameters that are safe from precision EW data and Run1 Tevatron constraints are $\Lambda_\phi = 5$ TeV ($\Rightarrow \hat{\Lambda}_W \sim 3$ TeV) and $m_0/M_{Pl} = 0.1$.

The latter $\Rightarrow m_1 \sim 780$ GeV; i.e. m_1 is typically too large for KK graviton excitations to be present, or if present, important, in h, ϕ decays.

- Given this choice, we complete the inversion by writing out the kinetic energy terms of the complete Lagrangian using the substitutions of Eqs. (4)

and (5) and demanding that the coefficients of $-\frac{1}{2}h^2$ and $-\frac{1}{2}\phi^2$ agree with the given input values for m_h^2 and m_ϕ^2 .

Results shown take $m_0/M_{Pl} = 0.1$.

- **KK excitation probably observable at LHC**

Will provide important information.

1. Mass gives m_1 in above notation.
2. Excitation spectrum as a function of m_{jj} determines m_0/M_{Pl} .
3. Combine ala Eq. (10) to get Λ_ϕ .

This will really help in LHC-only study of Higgs sector.

Apparently some work by B. Allanach and collaborators on accuracy with which Λ_ϕ can be determined.

The Couplings

The $f\bar{f}$ and VV couplings

- **The VV couplings**

- The h_0 has standard ZZ coupling.
- The ϕ_0 has ZZ coupling deriving from the interaction $-\frac{\phi_0}{\Lambda_\phi} T_\mu^\mu$ using the covariant derivative portions of $T_\mu^\mu(h_0)$.

The result for the $\eta_{\mu\nu}$ portion of the ZZ couplings is:

$$g_{ZZh} = \frac{g m_Z}{c_W} (d + \gamma b) , \quad g_{ZZ\phi} = \frac{g m_Z}{c_W} (c + \gamma a) . \quad (11)$$

g and c_W denote the $SU(2)$ gauge coupling and $\cos \theta_W$, respectively. The WW couplings are obtained by replacing gm_Z/c_W by gm_W .

- **The $f\bar{f}$ couplings**

- The h_0 has standard fermionic couplings.

- The fermionic couplings of the ϕ_0 derive from $-\frac{\phi_0}{\Lambda_\phi} T_\mu^\mu$ using the Yukawa interaction contributions to T_μ^μ .
- One obtains results in close analogy to the VV couplings just considered:

$$g_{f\bar{f}h} = -\frac{g m_f}{2 m_W}(d + \gamma b), \quad g_{f\bar{f}\phi} = -\frac{g m_f}{2 m_W}(c + \gamma a). \quad (12)$$

- Note same factors for WW and $f\bar{f}$ couplings.

We define

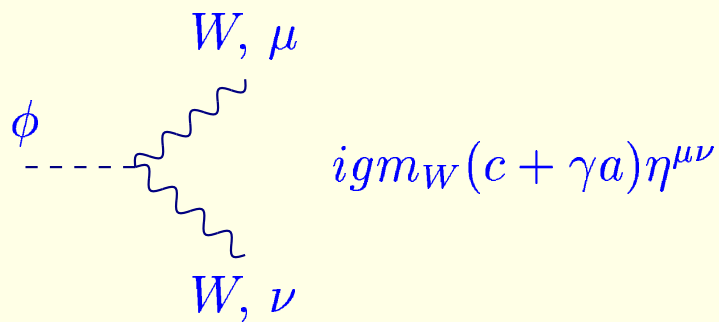
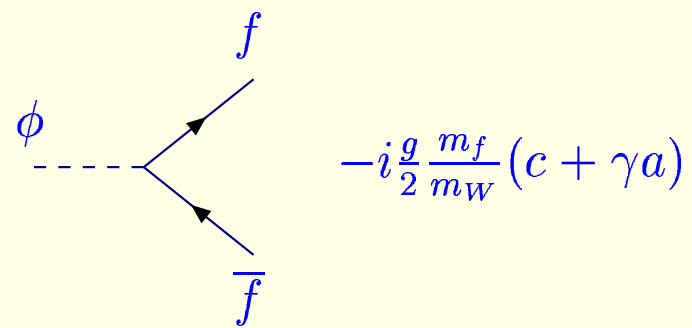
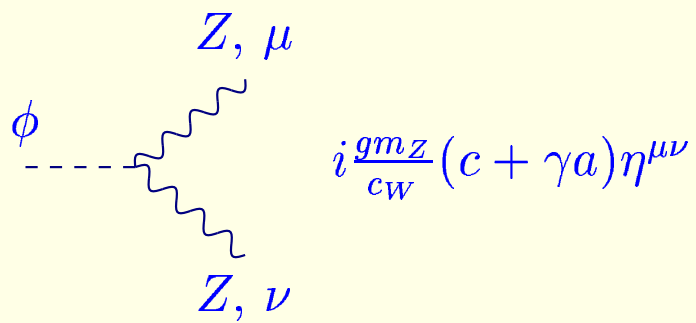
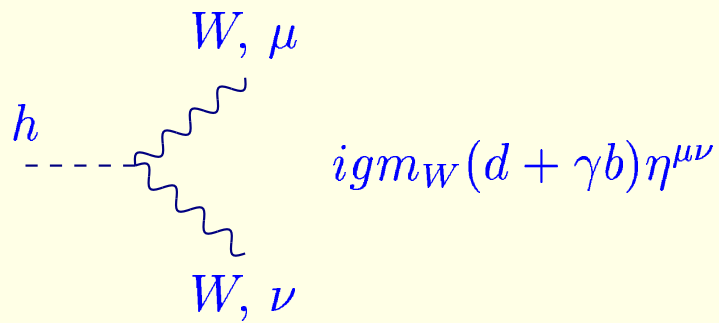
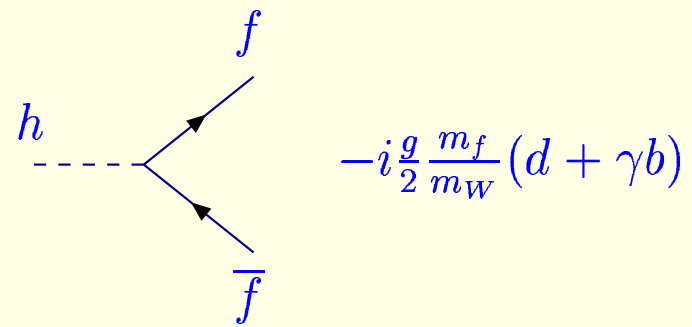
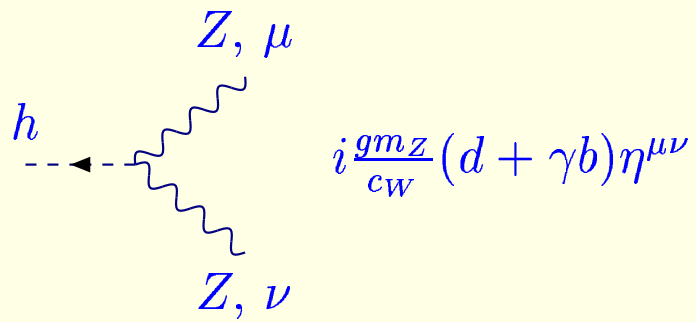
$$g_{fVh} \equiv d + \gamma b; \quad g_{fV\phi} \equiv c + \gamma a; \quad (13)$$

- There is a sum rule:

$$g_{fVh}^2 + g_{fV\phi}^2 = R^2; \quad R^2 = 1 + \frac{\gamma^2(1 - 6\xi)^2}{Z^2} \quad (14)$$

which says that $g_{fV\phi}^2$ must be at least as large as $1 - g_{fVh}^2$.

R^2 can't be too large without problems with precision electroweak, but it can certainly be somewhat larger than 1.

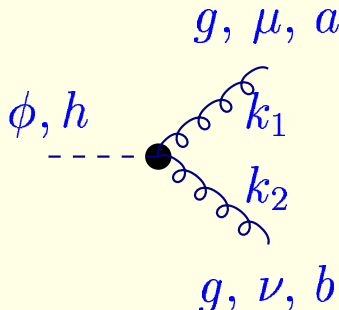


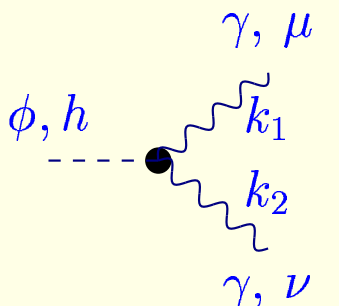
The gg and $\gamma\gamma$ couplings

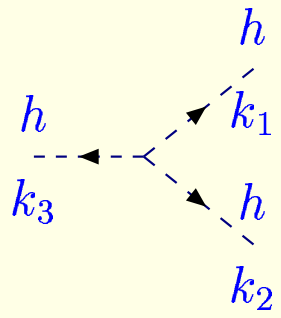
- There are the standard loop contributions, except rescaled by $f\bar{f}/VV$ strength factors g_{fVh} or $g_{fV\phi}$.
- In addition, **there are anomalous contributions**, which are expressed in terms of the $SU(3)\times SU(2)\times U(1)$ β function coefficients $b_3 = 7$, $b_2 = 19/6$ and $b_Y = -41/6$.
- **The anomalous couplings of h and ϕ enter only through their radion admixtures**, $g_h = \gamma b$ for the h , and $g_\phi = \gamma a$ for the ϕ .

The cubic interactions

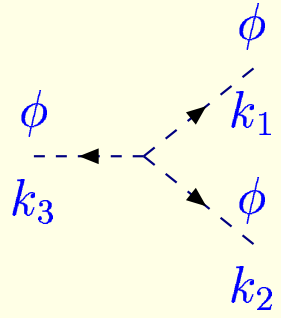
- There are four major sources of cubic interactions involving the h , the ϕ and the KK gravitons.
- **For $\xi \neq 0$** , they can lead to $h \rightarrow \phi\phi$ decays or the reverse $\phi \rightarrow hh$ decays. The $h \rightarrow \phi\phi$ decays typically have small BR for light h . $BR(\phi \rightarrow hh)$ can be substantial if the ϕ is heavy.

g, μ, a

 $i c_g \delta^{ab} [k_1 \cdot k_2 \eta^{\mu\nu} - k_1^\nu k_2^\mu] : c_g = -\frac{\alpha_s}{4\pi v} [g_{fV} \sum_i F_{1/2}(\tau_i) - 2b_3 g_r]$
 g, ν, b

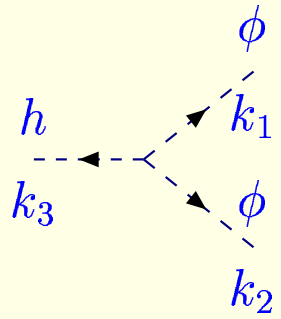
γ, μ

 $i c_\gamma [k_1 \cdot k_2 \eta^{\mu\nu} - k_1^\nu k_2^\mu] : c_\gamma = -\frac{\alpha}{2\pi v} [g_{fV} \sum_i e_i^2 N_c^i F_i(\tau_i) - (b_2 + b_Y) g_r]$
 γ, ν



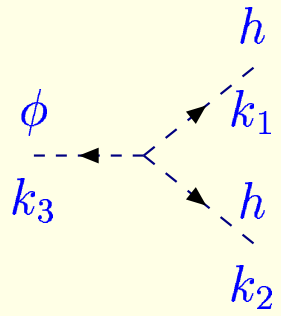
$$i \frac{g_{hhhh}}{\Lambda_\phi} \equiv \frac{i}{\Lambda_\phi} \left[bd \left\{ [12b\gamma\xi + d(6\xi + 1)] (k_1^2 + k_2^2 + k_3^2) - 12dm_{h_0}^2 \right\} - 3\gamma^{-1}d^3m_{h_0}^2 \right]$$



$$i \frac{g_{\phi\phi\phi}}{\Lambda_\phi} \equiv \frac{i}{\Lambda_\phi} \left[ac \left\{ [12a\gamma\xi + c(6\xi + 1)] (k_1^2 + k_2^2 + k_3^2) - 12cm_{h_0}^2 \right\} - 3\gamma^{-1}c^3m_{h_0}^2 \right]$$



$$i \frac{g_{\phi\phi\phi h}}{\Lambda_\phi} \equiv \frac{i}{\Lambda_\phi} \left[\left\{ 6a\xi(\gamma(ad + bc) + cd) + bc^2 \right\} (k_1^2 + k_2^2) + c \left\{ 12ab\gamma\xi + 2ad + bc(6\xi - 1) \right\} k_3^2 - 4c(2ad + bc)m_{h_0}^2 - 3\gamma^{-1}c^2dm_{h_0}^2 \right]$$

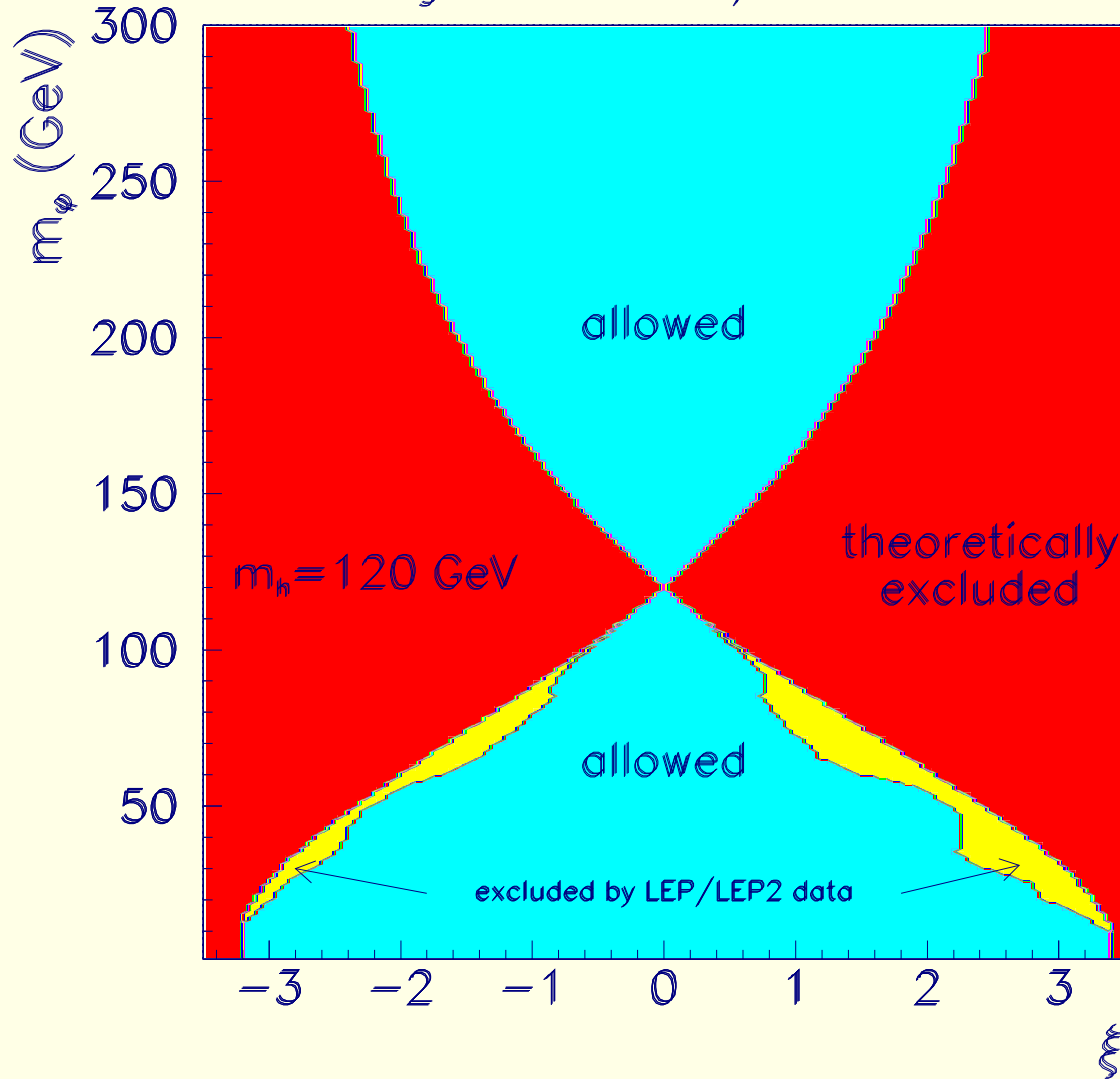


$$i \frac{g_{\phi\phi hh}}{\Lambda_\phi} \equiv \frac{i}{\Lambda_\phi} \left[\left\{ 6b\xi(\gamma(ad + bc) + cd) + ad^2 \right\} (k_1^2 + k_2^2) + d \left\{ 12ab\gamma\xi + 2bc + ad(6\xi - 1) \right\} k_3^2 - 4d(ad + 2bc)m_{h_0}^2 - 3\gamma^{-1}cd^2m_{h_0}^2 \right]$$

Constraints from LEP/LEP2

- To illustrate, temporarily choose $\Lambda_\phi = 5 \text{ TeV}$, i.e. $\gamma \sim 0.05$.
 $Z^2 > 0$ gives ξ constraint.
The mass difference $|m_h - m_\phi|$ increases with $|\xi|$ (because of requirement for successful inversion back to h_0, ϕ_0 basis).
Exact results very sensitive to including all kinetic energy terms in the h_0, ϕ_0 basis.
- LEP/LEP2 provides an upper limit on ZZs ($s = h$ or ϕ) from which we can exclude regions in the (m_h, m_ϕ) plane for a given choice of R^2 .
Use upper limits on the ZZs coupling in both with and without b tagging, with computed branching ratios into b and non- b final states.
- **Conclusions:**
Small m_ϕ relative to m_h is entirely possible given current data so long as $m_h \gtrsim 115 \text{ GeV}$. (The $ZZ\phi$ coupling does not blow up.)
 $m_\phi > m_h$ is also possible, but to avoid conflict with precision electroweak data $g_{ZZ\phi}$ must not be too large if m_ϕ is large.

Allowed Regions and LEP/LEP2 Constraints



Couplings

- First, consider the $f\bar{f}/VV$ couplings of h and ϕ relative to SM, taking $m_h = 120$ GeV and $\Lambda_\phi = 5$ TeV.

- The most important points

If $g_{fVh}^2 < 1$ is observed then $m_\phi > m_h$, and vice versa, except for small region near $\xi = 0$.

In cases where $g_{fV\phi}$ is small, prior indirect knowledge of, or constraints on, m_ϕ could be crucial.

At large $|\xi|$, if $m_\phi > m_h$ the $ZZ\phi$ couplings can become sort of SM strength, implying SM type discovery modes could become relevant.

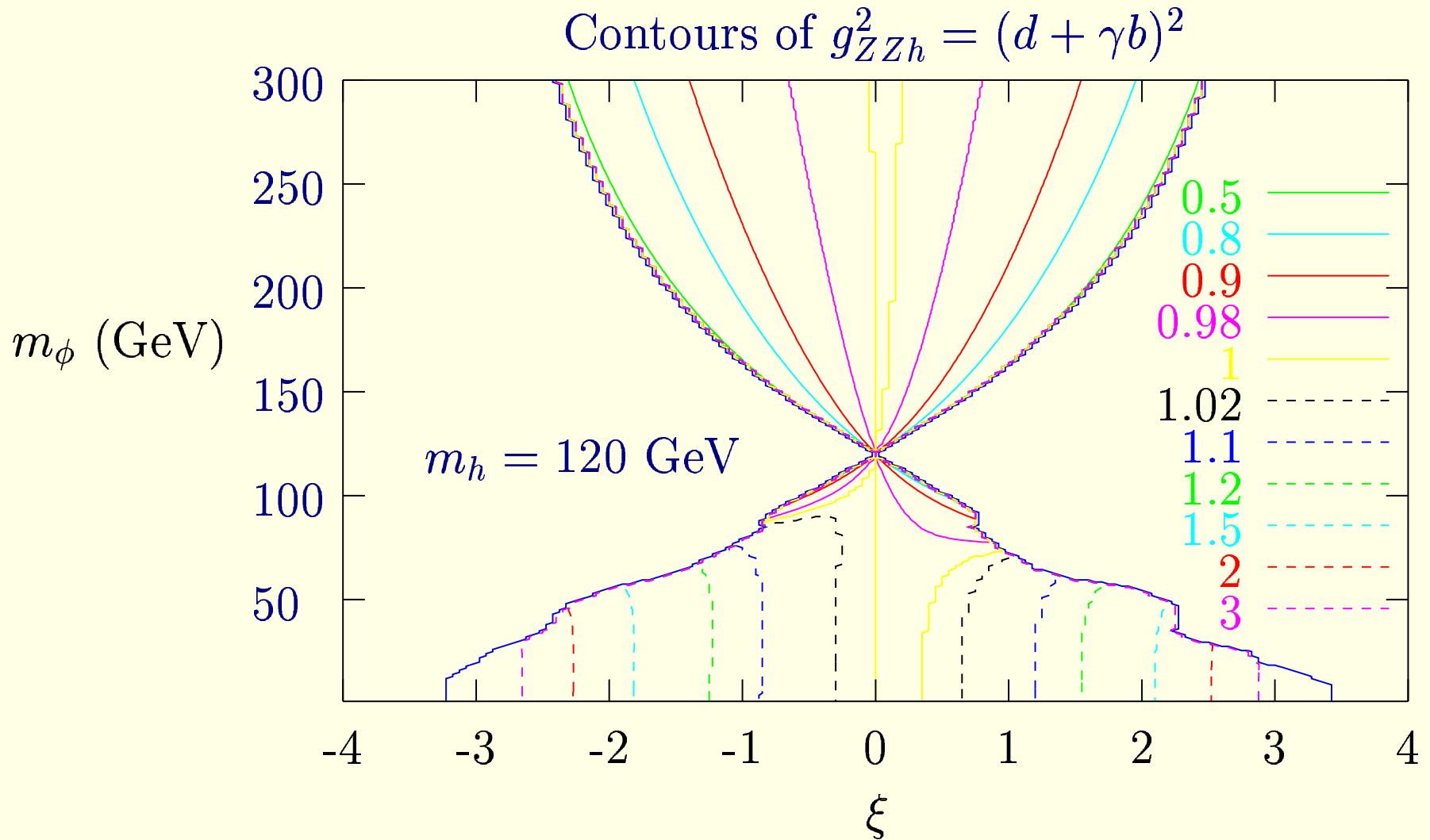


Figure 1: Contours of g_{fVh}^2 (relative to SM) for $\Lambda_\phi = 5 \text{ TeV}$, $m_h = 120 \text{ GeV}$.

- Observe suppression if $m_\phi > m_h$ and vice versa.

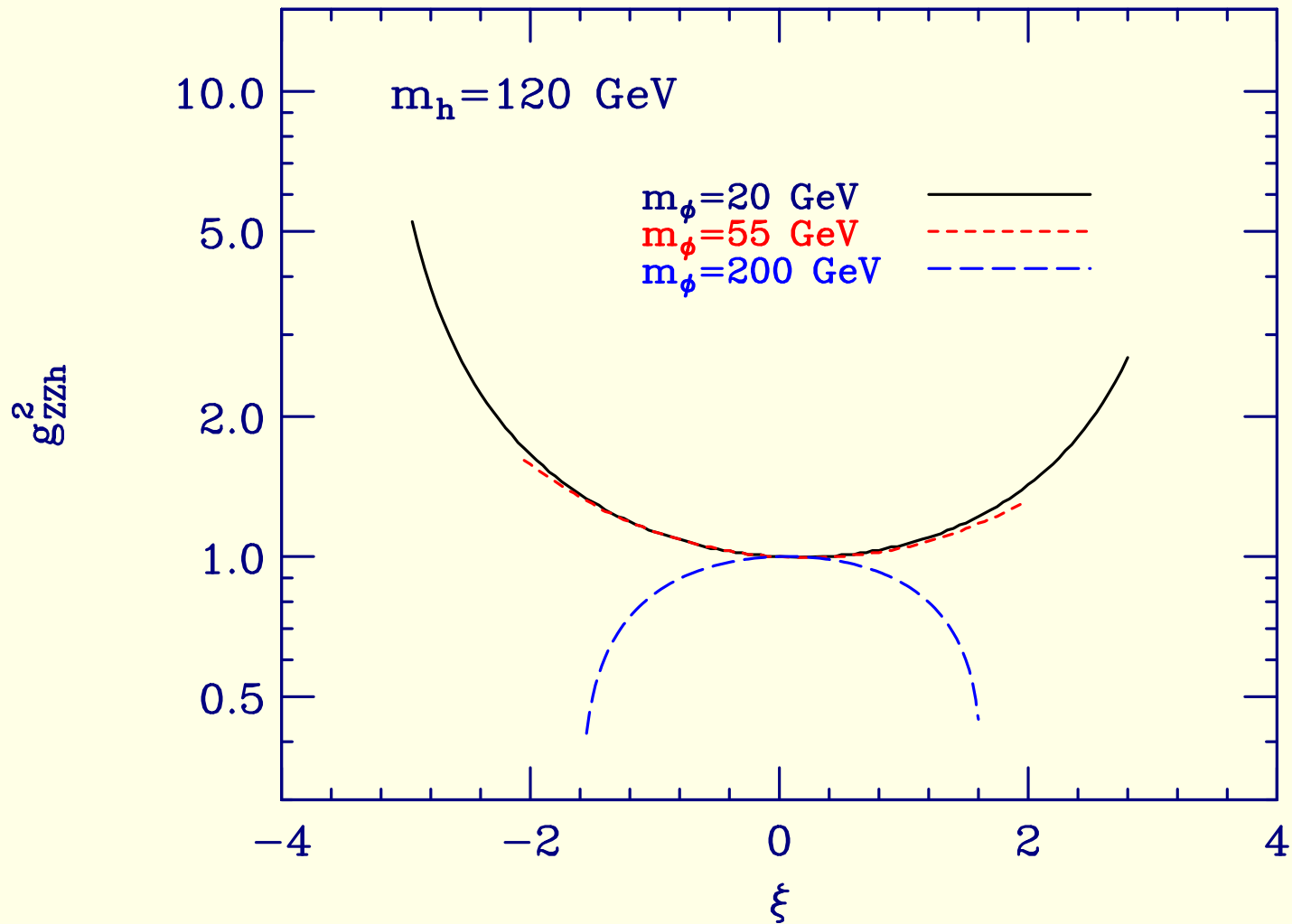


Figure 2: $g_{ZZh}^2/g_{ZZh_{SM}}^2 = g_{f\bar{f}h}^2/g_{f\bar{f}h_{SM}}^2$ as a function of ξ for several m_ϕ values.

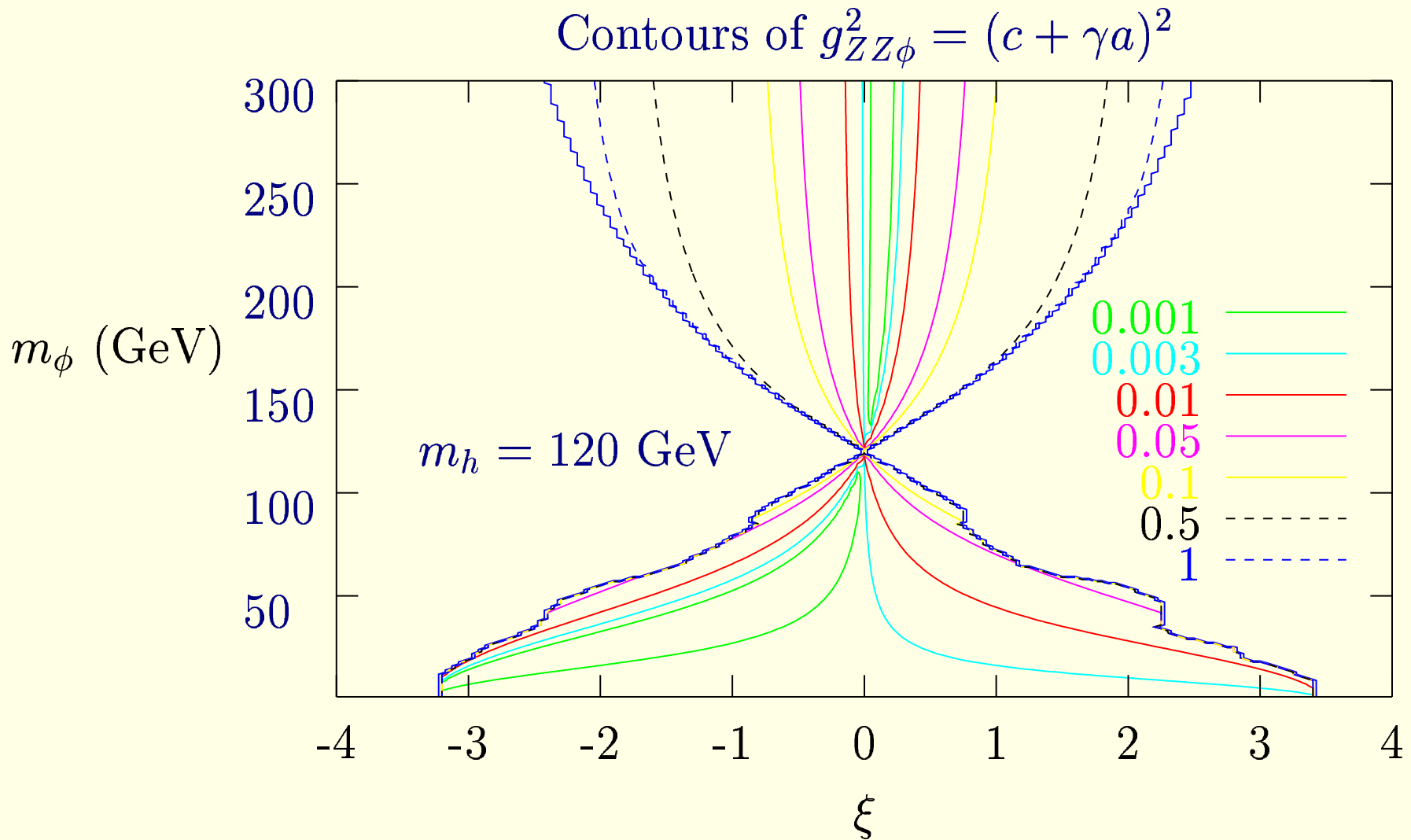


Figure 3: Contours of $g_{fV\phi}^2$ for $\Lambda_\phi = 5 \text{ TeV}$, $m_h = 120 \text{ GeV}$

- Substantial $g_{fV\phi}^2$ is possible if $m_\phi > m_h$ and ξ is not too small.

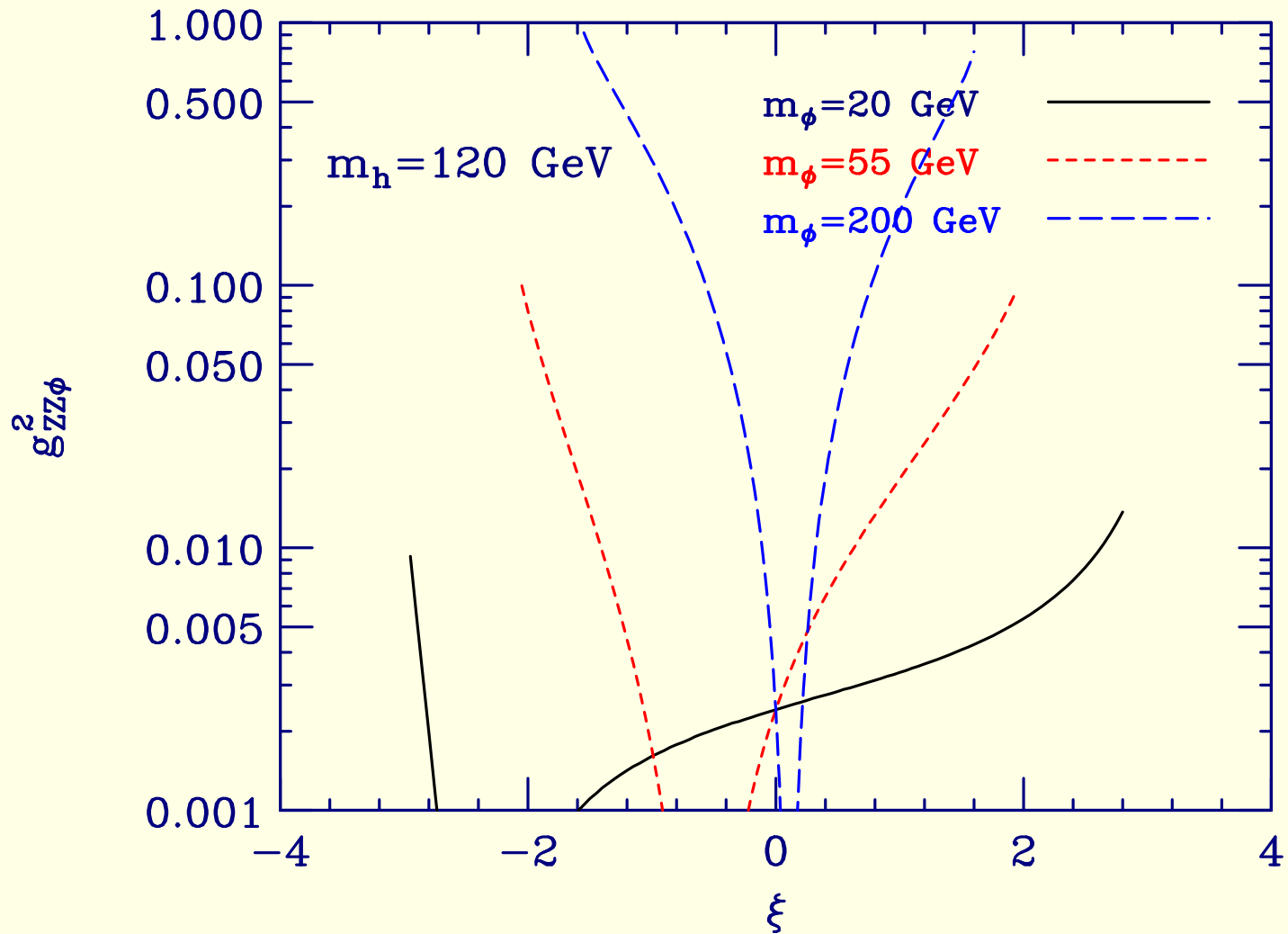


Figure 4: $g_{ZZ\phi}^2/g_{ZZh_{SM}}^2 = g_{f\bar{f}\phi}^2/g_{f\bar{f}h_{SM}}^2$ as a function of ξ for several m_ϕ values.

Branching Ratios

Some important points are:

- h branching ratios are quite SM-like (even if partial widths are different) except that $h \rightarrow gg$ can be bigger than normal, especially when g_{fVh}^2 is suppressed.
- For $m_\phi < 2m_W$, $\phi \rightarrow gg$ is very possibly the dominant mode in the substantial regions near zeroes of $g_{fV\phi}^2$.

For $m_\phi > 2m_W$, ϕ branching ratios are sort of SM-like (except at $\xi \simeq 0$) but total and partial widths are rescaled.

Precision Electroweak Constraints

- There was considerable work on this in the past, but we (JFG, Toharia, Wells) claim there were some inaccuracies ... and we have done a very careful analysis.
- One of our important new ingredients is a metric that solves the Einstein equations to 2nd order in the radion field expansion. This fixes some important components related to quartic couplings that contribute to the W and Z propagator corrections.
- One of the issues that one must address is certain model-dependent anomalous contributions. However, the precision constraints are most interesting when $|\xi|$ is near its upper limits. In this case, these and other model-dependent terms associated with KK exchanges are quite small compared to the mixing effects.

For example, in the Hewett-Rizzo analysis, they conclude that precision electroweak data is sensitive to Λ_ϕ up to 1.8 TeV (or lower). So, for our

typical case of $\Lambda_\phi = 5$ TeV or higher, the radion-Higgs sector is the only important one.

If ξ is small, the KK influence and radion-Higgs stuff both are both small when m_h is in the $\lesssim 150$ GeV domain.

If $m_h > 211$ GeV, precision electroweak requires large ξ in order to regain consistency. KK influence will not be significant unless $\Lambda_\phi \lesssim 2$ TeV.

- One important result is that portions of the parameter space illustrated earlier for $m_h = 120$ GeV are excluded by the precision electroweak analysis.

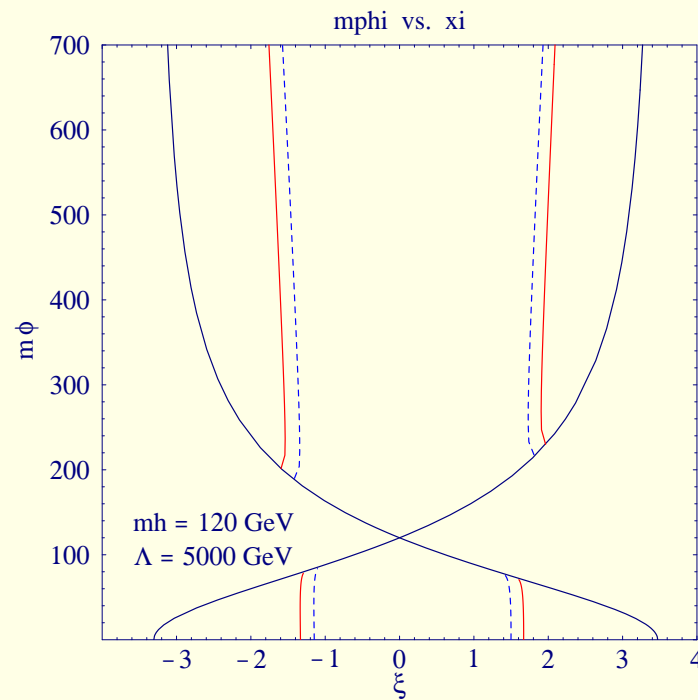


Figure 5: Typical constraint on m_ϕ , ξ parameter space for $m_h = 120$ GeV. 95% and 99% CL contours are shown.

- Another important result, is that m_h and m_ϕ can both be quite large without violating precision electroweak constraints, so long as $|\xi|$ is large

enough.

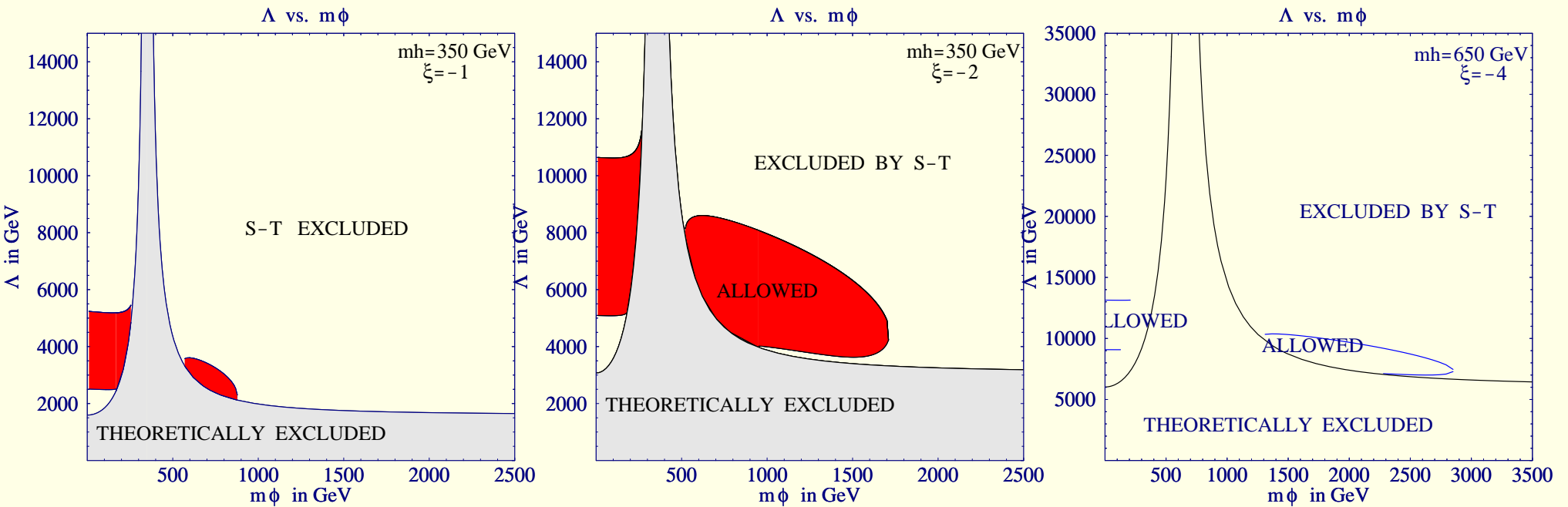


Figure 6: Illustration of how modest ξ values allow region for which m_h and m_ϕ are both relatively large.

- Another important result, is that m_h and m_ϕ can both be quite large

without violating precision electroweak constraints, so long as $|\xi|$ is large enough.

This is possible without violating precision electroweak constraints because the radion contributions compensate the Higgs contributions in the S, T plane. But, note that this is only possible if Λ is not too large (so that the radion does not decouple as it does as $\Lambda \rightarrow \infty$).

In this domain of parameter space, one will have to move the LC to higher \sqrt{s} or look carefully at the LHC sensitivity to the higher mass h and ϕ . This has not been done yet.

An example of LHC/LC Complementarity

We (Battaglia, Dominici, de Curtis, de Roeck, JFG) focused on the case of a relatively light Higgs boson, $m_h = 120$ GeV for example.

- The precision EW studies suggest that some of the larger $|\xi|$ range is excluded, but we studied the whole range just in case.
- We rescaled the statistical significances predicted for the SM Higgs boson at the LHC using the h and ϕ couplings predicted relative to the h_{SM} .

A modified version of HDECAY was employed.

- The most important modes are $gg \rightarrow h \rightarrow \gamma\gamma$ and $gg \rightarrow \phi \rightarrow ZZ^{(*)} \rightarrow 4\ell$.

Also useful are $t\bar{t}h$ with $h \rightarrow b\bar{b}$ and $h \rightarrow ZZ^* \rightarrow 4\ell$.

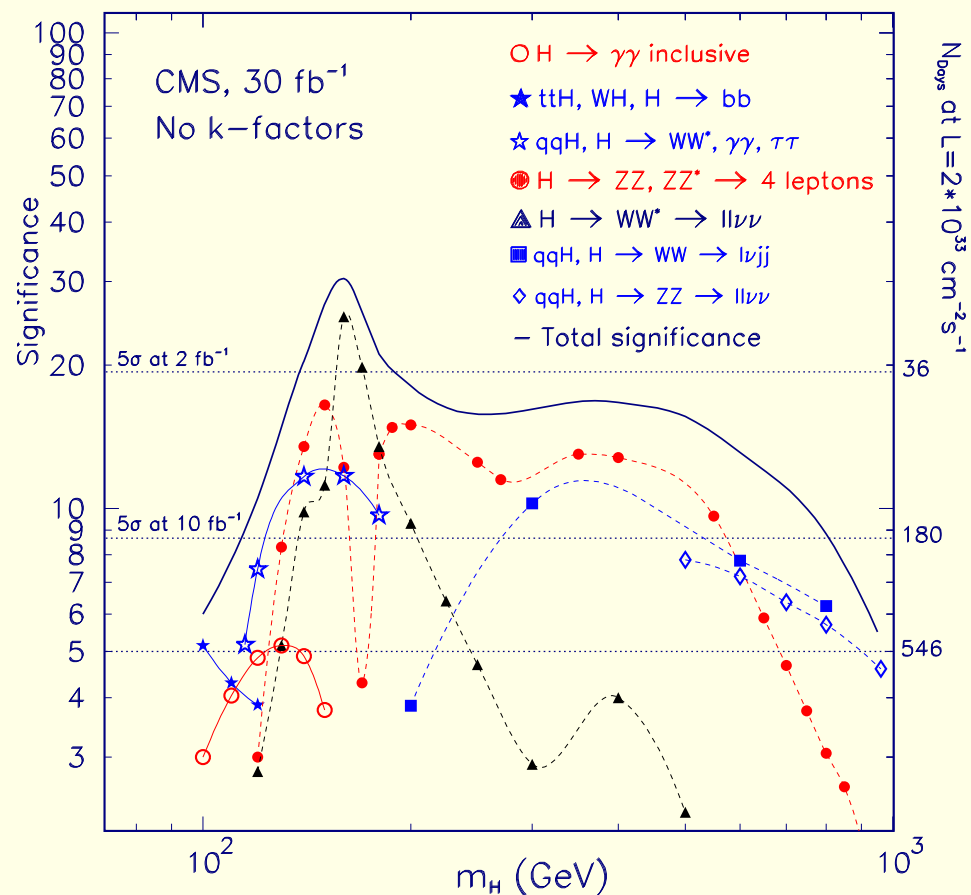
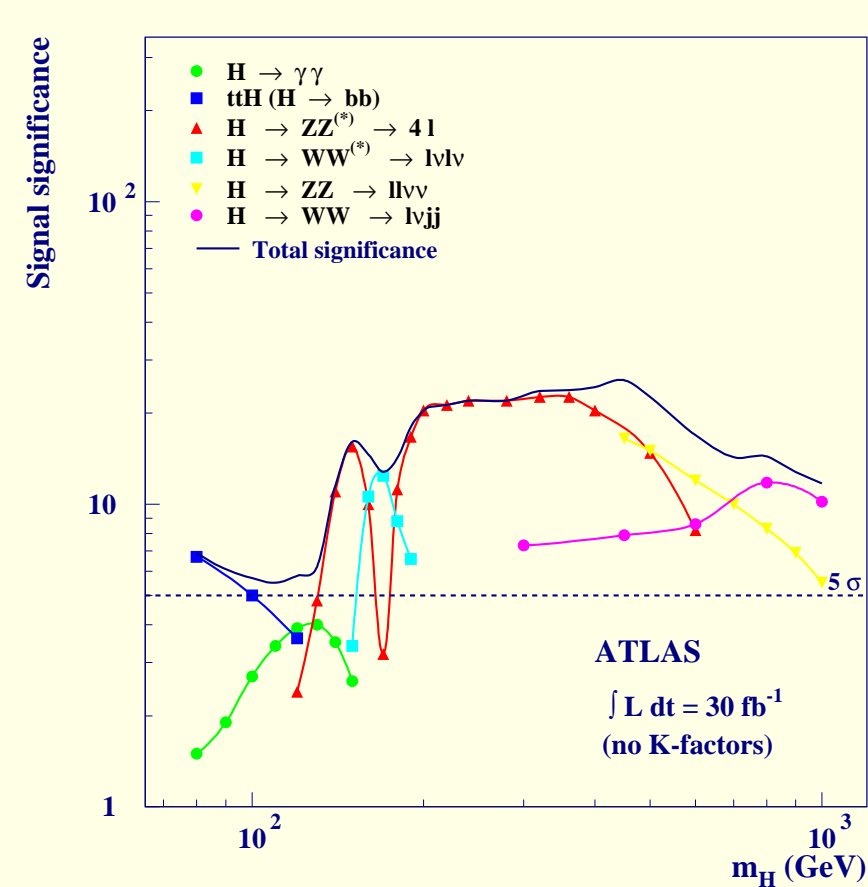


Figure 7: SM Higgs search capabilities at the LHC for ATLAS and CMS.

- An example of the type of effect that will be observed is that the $h \rightarrow \gamma\gamma$ mode becomes unobservable if $|\xi|$ is large and $m_\phi > m_h$ (which together imply suppressed hWW coupling and hence suppressed W -loop

contribution to the $\gamma\gamma h$ couplings).

One interesting graph is below. Note how we lose the $h \rightarrow \gamma\gamma$ mode if $m_\phi > m_h$, especially if $\xi < 0$. If $m_\phi < m_h$, $h \rightarrow \gamma\gamma$ will be strong if $\xi < 0$, but can be considerably weakened if $\xi > 0$.

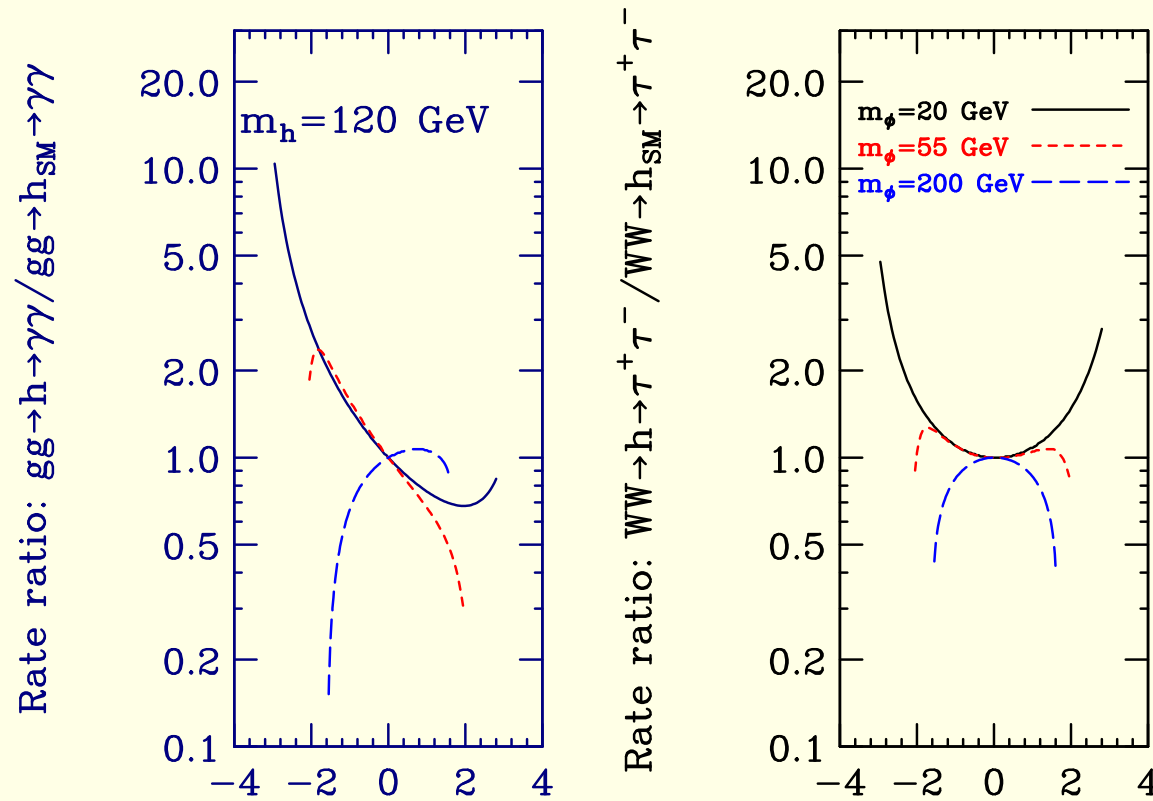


Figure 8: $gg \xrightarrow{\xi} h \rightarrow \gamma\gamma / gg \xrightarrow{\xi} h_{SM} \rightarrow \gamma\gamma$ and $WW \rightarrow h \rightarrow \tau^+ \tau^- / WW \rightarrow h_{SM} \rightarrow \tau^+ \tau^-$ (same as for $gg \rightarrow t\bar{t}h \rightarrow t\bar{t}b\bar{b}$) for $m_{h_{SM}} = m_h$; $\Lambda_\phi = 5 \text{ TeV}$.

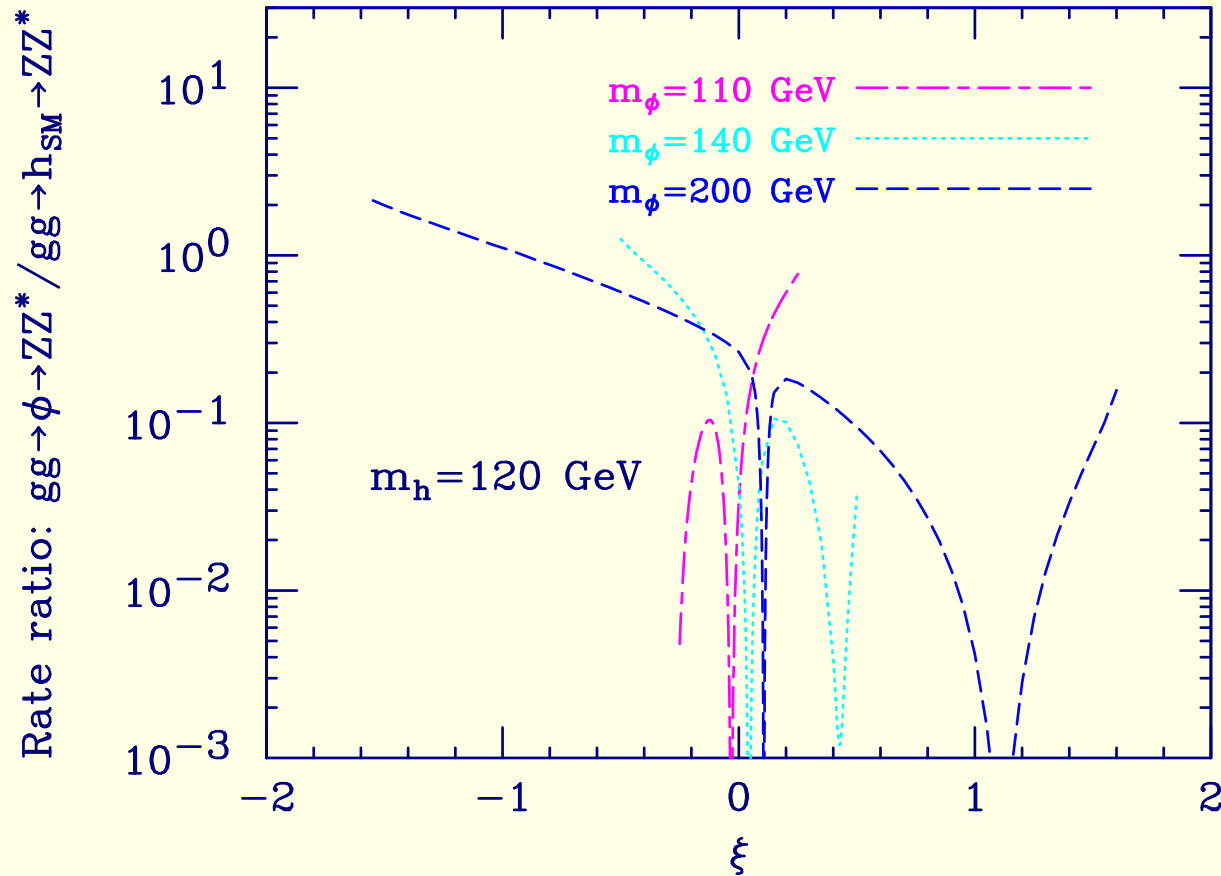


Figure 9: The ratio of the rate for $gg \rightarrow \phi \rightarrow ZZ$ to the corresponding rate for a SM Higgs boson with mass m_ϕ assuming $m_h = 120$ GeV and $\Lambda_\phi = 5$ TeV as a function of ξ for $m_\phi = 110, 140$ and 200 GeV. Recall that the ξ range is increasingly restricted as m_ϕ becomes more degenerate with m_h . *Note:* for $m_\phi > m_h$ the mode approaches SM strength if $\xi < 0$ and is nearing SM strength if $\xi > 0$ and near maximal.

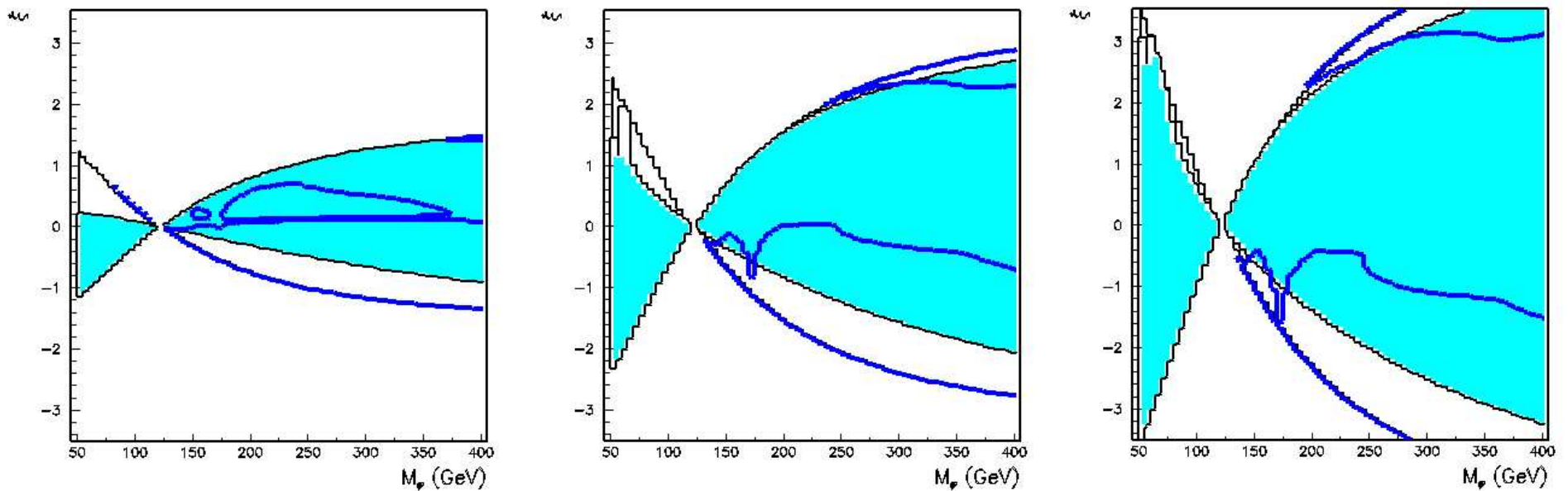


Figure 10: $L = 30\text{fb}^{-1}$ illustration of mode complementarity at the LHC for $m_h = 120$ GeV. The cyan regions show where the $gg \rightarrow h \rightarrow \gamma\gamma$ mode (or not very important at this m_h value, $gg \rightarrow h \rightarrow 4\ell$ mode) yields a $> 5\sigma$ signal. The regions between dark blue curves define the regions where $gg \rightarrow \phi \rightarrow 4\ell$ is $> 5\sigma$. The graphs are for $\Lambda_\phi = 2.5$ TeV (left) $\Lambda_\phi = 5$ TeV (center) and $\Lambda_\phi = 7.5$ TeV (right).

The LHC is doing pretty well except for the $m_\phi < m_h$, $\xi > 0$ and large, region.

But, some portion of this difficult region is disfavored by the precision electroweak data — e.g. $|\xi| \lesssim 1.5$ in the $\Lambda_\phi = 5$ TeV case.

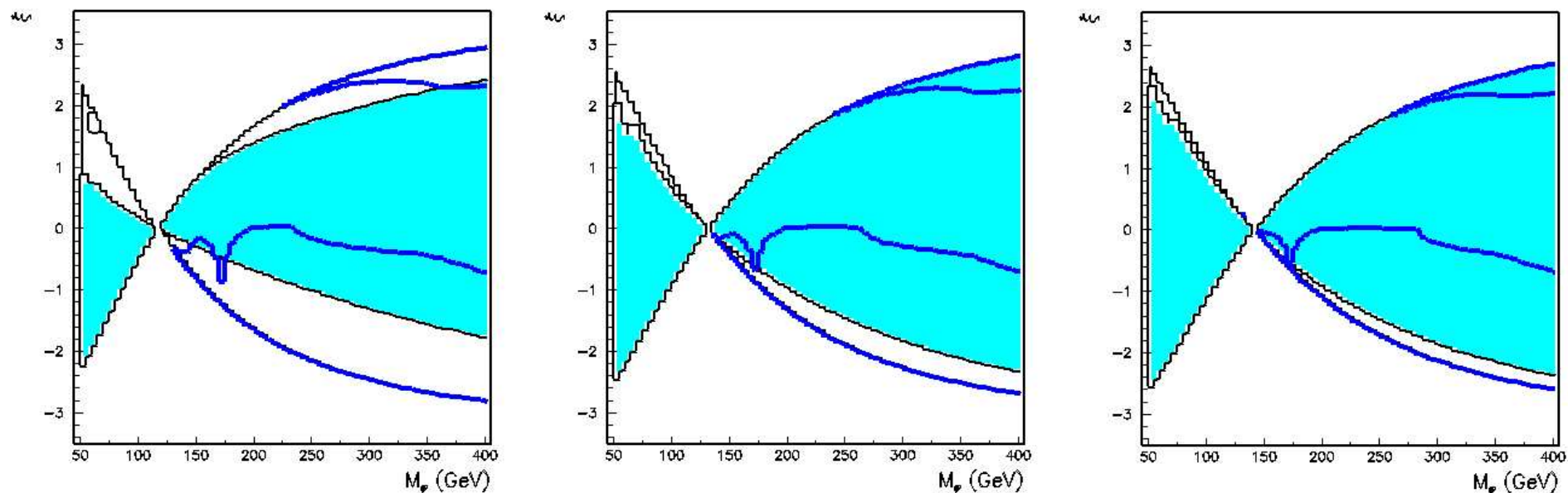


Figure 11: As in previous figure. The graphs are for $\Lambda_\phi = 5$ TeV and $m_h = 115$ GeV (left) $m_h = 130$ GeV (center) and $m_h = 140$ GeV (right).

Above, we see that the region where neither the h nor the ϕ can be detected grows (decreases) as m_h decreases (increases). It diminishes as m_h increases since the $gg \rightarrow h \rightarrow 4\ell$ increases in strength at higher m_h .

The regions where the h is not observable are reduced by considering either a larger data set or qqh Higgs production, in association with forward jets. An integrated luminosity of 100 fb^{-1} would remove the regions at large positive ξ in the $\Lambda_\phi = 5$ and 7.5 TeV plots of Fig. 10. Similarly,

including the $q\bar{q}h$, $h \rightarrow WW^* \rightarrow \ell\nu\bar{\nu}$ channel in the list of the discovery modes removes the same two regions and reduces the large region of h non-observability at negative ξ values.

- We should also note that the $\phi \rightarrow Z^0 Z^0$ decay is reduced for $m_\phi > 2m_h$ by the onset of the $\phi \rightarrow hh$ decay, which can become the main decay mode. The resulting $hh \rightarrow b\bar{b}b\bar{b}$ topology, with di-jet mass constraints, may represent a viable signal for the LHC in its own right, but detailed studies will be needed.
- Figures 10 and 11 also exhibit regions of (m_h, ξ) parameter space in which both the h and ϕ mass eigenstates will be detectable.

In these regions, the LHC will observe two scalar bosons somewhat separated in mass, with the lighter (heavier) having a non-SM-like rate for the gg -induced $\gamma\gamma$ ($Z^0 Z^0$) final state.

Additional information will be required to ascertain whether these two Higgs bosons derive from a multi-doublet or other type of extended Higgs sector or from the present type of model with Higgs-radion mixing.

- An e^+e^- LC should guarantee observation of both the h and the ϕ in the

region of low m_ϕ , large $\xi > 0$ within which detection of either at the LHC might be difficult. This is because the $ZZ\phi$ coupling-squared is $\gtrsim 0.01$ relative to the SM for most of this region.

Thus, this scenario provides another illustration of the complementarity between the two machines in the study of the Higgs sector.

- In particular, Figs. 1 and 2 show:
 - * In the region with $m_\phi > m_h$ the hZ^0Z^0 coupling is enhanced relative to the SM $h_{\text{SM}}Z^0Z^0$ coupling and h detection in e^+e^- collisions would be even easier than SM h_{SM} detection.
 - * Even in the $m_\phi < m_h$ part of parameter space, $g_{hZZ}^2 \geq 0.5g_{h_{\text{SM}}ZZ}^2$, a level for which the h would be easily seen at the LC.
- Further, assuming that e^+e^- collisions could also probe down to ϕZ^0Z^0 couplings of order $g_{\phi ZZ}^2/g_{h_{\text{SM}}ZZ}^2 \simeq 0.01$, the ϕ would be seen in almost the entirety of the $m_\phi > m_h$ region for which ϕ detection at the LHC would not be possible. In particular, from Figs. 3 and 4 we find that the only regions where the ϕ could not be observed in e^+e^- collisions are:
 - * a) near the very narrow 0 in $g_{ZZ\phi}^2$ for $\xi \sim 0 \div 1/6$ in the $m_\phi > m_h$ region;
 - * b) for significant portions of the $m_\phi < m_h$ region where the $ZZ\phi$ coupling tends to be rather suppressed on average.

However, the $m_\phi < m_h$ large $\xi > 0$ region will for the most part yield an observable signal (assuming expected LC luminosity).

- Where both the h and ϕ can be seen, the measurements of the $Z^0 Z^0$ boson couplings of both the Higgs and the radion particles would significantly constrain the values of the ξ and Λ_ϕ parameters of the model.

Ultimately, having these two measurements is absolutely crucial to really pinning down the model.

Determining the Nature of the Observed Scalar

The interplay between the emergence of the Higgs boson and of the radion graviscalar signals opens up the question of the identification of the nature of the newly observed particle(s).

After observing a new scalar at the LHC, some of its properties will be measured with sufficient accuracy to determine if they correspond to those expected for the SM h_{SM} , i.e. for the minimal realization of the Higgs sector — see Zeppenfeld et al.

In the presence of extra dimensions, further scenarios emerge. For the present discussion, we consider two scenarios.

1. The first has a light Higgs boson, for which we take $m_h = 120$ GeV, with couplings different from those predicted in the SM.

The question here is if the anomaly is due to an extended Higgs sector, such as in Supersymmetry, or rather to the mixing with an undetected radion.

2. The second scenario consists of an intermediate-mass scalar, with $180 \text{ GeV} < M < 300 \text{ GeV}$, observed alone.

An important issue would then be the question of whether the observed particle is the SM-like Higgs boson or a radion, with the Higgs particle left undetected.

The “radion alone” scenario is quite likely at large negative ξ and large m_ϕ — see Figures 10 and 11.

- Case 1

In the first scenario, the issue is the interpretation of discrepancies in the measured Higgs couplings to gauge bosons and fermions.

These effects increase with $|\xi|$, $1/\Lambda_\phi$ and m_h/m_ϕ .

The LHC is expected to measure some ratios of these couplings.

In the case of the SM h_{SM} , the ratio $g_{h_{\text{SM}}ZZ}/g_{h_{\text{SM}}WW}$ can be determined with a relative accuracy of 15% to 8% for $120 \text{ GeV} < m_{h_{\text{SM}}} < 180 \text{ GeV}$, while the ratio $g_{h_{\text{SM}}\tau\tau}/g_{h_{\text{SM}}WW}$ and that of the effective coupling to photons, $g_{h_{\text{SM}}\gamma\gamma}^{\text{effective}}/g_{h_{\text{SM}}WW}$ can be determined to 6% to 10% for $120 \text{ GeV} < m_{h_{\text{SM}}} < 150 \text{ GeV}$.

Now, the Higgs-radion mixing would induce the same shifts in the direct

couplings g_{hWW} , g_{hZZ} and $g_{h\bar{f}f}$, all being given by $d + \gamma b$ times the corresponding h_{SM} couplings.

Although this factor depends on the Λ_ϕ , m_ϕ and ξ parameters, **ratios of couplings would remain unperturbed and correspond to those expected in the SM.**

To the extent that the LHC measures mostly ratios of couplings, the presence of Higgs-radion mixing could easily be missed.

One window of sensitivity to the mixing would be offered by the combination $g_{h\gamma\gamma}^{\text{effective}}/g_{hWW}$. But the mixing effects are expected to be limited to relative variation of $\pm 5\%$ w.r.t. the SM predictions.

Hence, the LHC anticipated accuracy corresponds to deviations of one unit of σ , or less, except for a small region at $\Lambda_\phi \simeq 1$ TeV.

Larger deviations are expected for the absolute rates, especially for the $gg \rightarrow h \rightarrow \gamma\gamma$ channel which can be dramatically enhanced or suppressed relative to the $gg \rightarrow h_{\text{SM}} \rightarrow \gamma\gamma$ prediction for larger ξ values due to the large changes in the $gg \rightarrow h$ and $h \rightarrow \gamma\gamma$ couplings relative to the h_{SM} couplings. See Fig. 8.

Of course, to detect these deviations it is necessary to control systematic

uncertainties for the absolute $\gamma\gamma$ rate.

All the above remarks would also apply to distinguishing between the light Higgs of supersymmetry, which would be SM-like assuming an approximate decoupling limit, and the h of the Higgs-radion scenario.

In a non-decoupling two-doublet model, the light Higgs couplings to up-type and down-type fermions can be modified differently with respect to those of the SM h_{SM} , and LHC measurements of coupling ratios would detect this difference.

A TeV-class LC has the capability of performing **absolute coupling measurements** (as opposed to ratio measurements as at the LHC) of all fermions separately with accuracies of order 1%-5% and achieves a determination of the total width to 4% - 6% accuracy.

This is important for the scenario we propose since it would provide enough measurements and sufficient accuracy to detect Higgs-radion mixing for moderate to large ξ values. This is shown in Figure 12 by the additional contours, which indicate the regions where the discrepancy with the SM predictions for the Higgs couplings to pairs of b quarks and W bosons exceeds 2.5σ .

In particular, the *combination* of the direct observation of $\phi \rightarrow Z^0 Z^{0*}$ at

the LHC and the precision measurements of the Higgs properties at a e^+e^- LC will extend our ability to distinguish between the Higgs-radion mixing scenario and the SM h_{SM} scenario to a large portion of the regions where at the LHC only the h or only the ϕ is detected and determining that the observed boson is not the SM h_{SM} is difficult.

Further, close to the edges of the hourglass-shaped allowed region, the LC will also be able to detect ϕ production directly through the process $e^+e^- \rightarrow Z^0\phi$. In particular, this process will guarantee the observability of the ϕ in the low m_ϕ region, which is most difficult for the LHC.

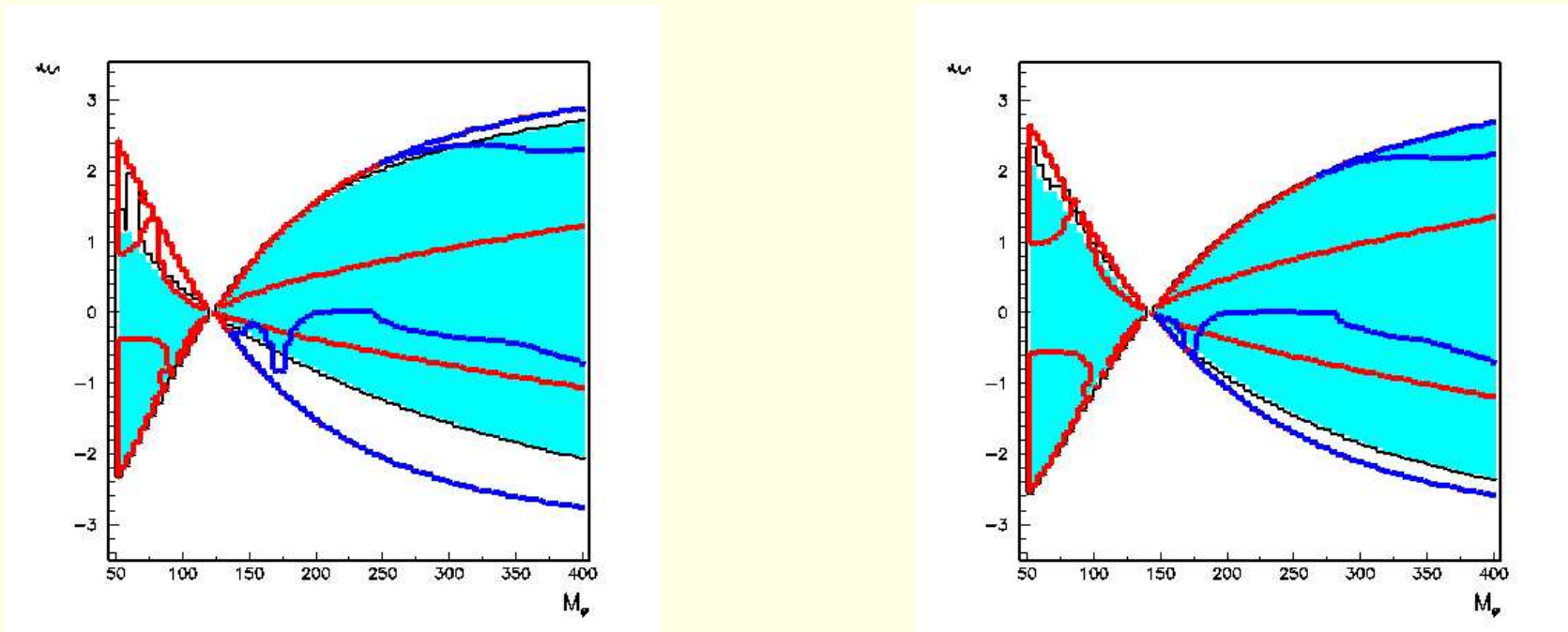


Figure 12: Same as Figures 10 and 11 for $m_h = 120$ GeV (left), 140 GeV (right) and $\Lambda_\phi = 5$ TeV with added contours, indicated by the medium gray (red) curves, showing the regions where the LC measurements of the h couplings to $b\bar{b}$ and W^+W^- would provide a $> 2.5 \sigma$ evidence for the radion mixing effect. (Note: the gray (red) lines are always present along the outer edge of the hourglass in the $m_\phi > m_h$ region, but are sometimes buried under the darker (blue) curves. In this region, the $> 2.5 \sigma$ regions lie between the outer hourglass edges and the inner gray (red) curves.)

- Case 2

If, at the LHC, an intermediate mass scalar is observed alone, its non-SM-like nature can, in some cases, be determined through measurement of its production yield and its couplings.

In particular, in the region at large, negative ξ values where ϕ production is visible whereas h production is not, the yield of $Z^0 Z^0 \rightarrow 4 \ell$ from ϕ decay can differ by a factor of 2 or more from that expected for a SM h_{SM} (depending upon the value of m_ϕ — see Figure 9.)

For m_ϕ such that $\phi \rightarrow hh$ decays are not allowed, the deviations arise from the substantial differences between the $gg \rightarrow \phi$ coupling and the $gg \rightarrow h_{\text{SM}}$ coupling.

For $m_\phi > 2m_h$ this rate is also sensitive to the exclusive branching fraction. Figure 13 shows the ratio of the $Z^0 Z^{0(*)}$ decay branching fraction for the radion to that for the SM h_{SM} . The figure shows that branching ratio differences are expected to be below 10% for radions with mass up to twice the Higgs mass. Such a small difference would not have a big impact compared to the possibly large deviations of $gg \rightarrow h/gg \rightarrow h_{\text{SM}}$ relative to unity.

However, past the threshold for $\phi \rightarrow hh$ decays, the $Z^0 Z^0$ branching fraction is significantly affected away from $\xi \simeq 0$. The combination of a reduced $Z^0 Z^0 \rightarrow 4 \ell$ rate and the possibility to observe $\phi \rightarrow hh$ decays, ensures that the LHC could positively identify the existence of the radion in the region $m_\phi > 2m_h$, $\xi \neq 0$.

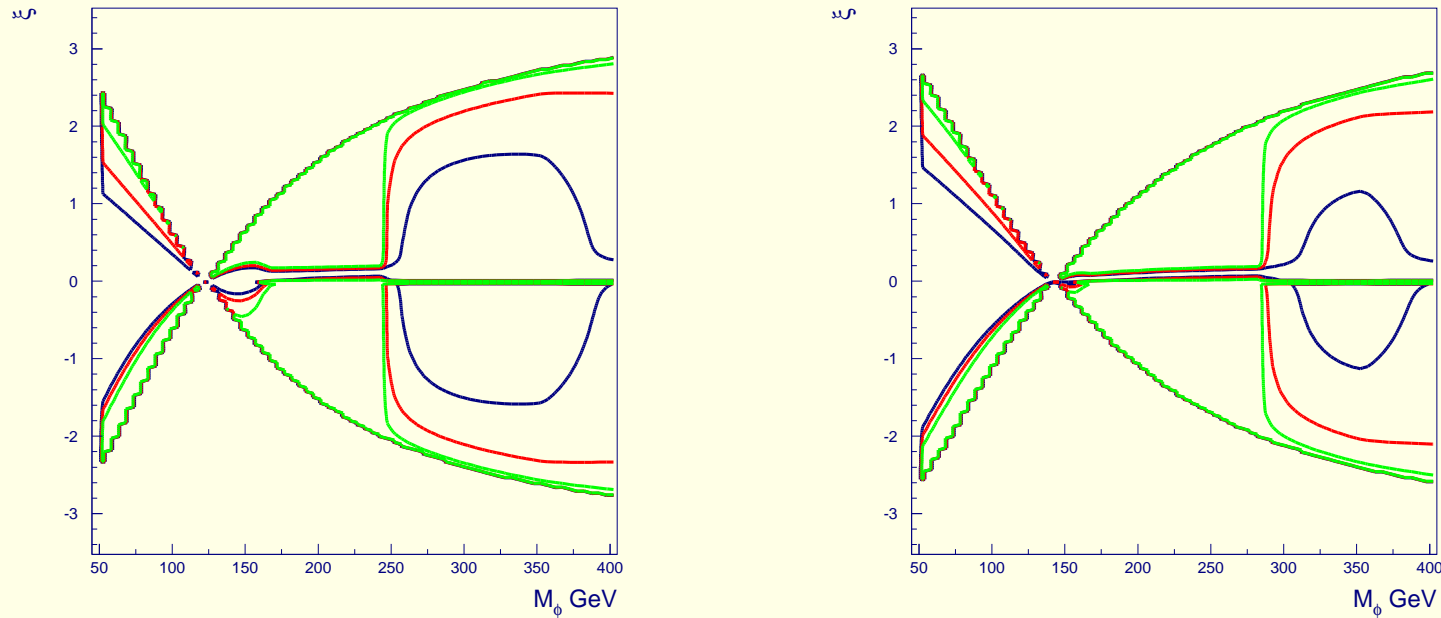


Figure 13: Ratio $\frac{\text{BR}(\phi \rightarrow Z^0 Z^{0(*)})}{\text{BR}(h_{\text{SM}} \rightarrow Z^0 Z^{0(*)})}$ as function of m_ϕ and ξ . The curves indicate the 0.7 (black), 0.8 (medium gray/red) and 0.9 (light gray/green) contours. Results are obtained for $m_h=120$ GeV (left) and $m_h = 140$ GeV (right) and $\Lambda_\phi=5.0$ TeV. The radion can be distinguished from the SM Higgs particle at intermediate values of its mass, past the threshold for the $\phi \rightarrow hh$ decay.

New Ideas

- Determining that there is an anomalous ggh coupling
- Return to scenario where we see a light h , but do not necessarily see the ϕ . How can you test for a radion-Higgs scenario using just h information from the LHC.
 1. If you see the first KK excitation, and it fits the RS expectation, you will have a first strong hint for the RS scenario.
You will know m_1 and the resonance shape will strongly constrain m_0/M_{P} . Then some approximate value of Λ_ϕ will be determined. Suppose it is our favorite value of $\Lambda_\phi = 5 \text{ TeV}$.
 2. An interesting case is if we see the $gg \rightarrow h \rightarrow \gamma\gamma$ mode.
It will depend on ξ and other parameters of the model. But, deviation of this rate from the SM prediction could be explained by extended models other than Higgs-radion mixing.
 3. Given the improved results for the $t\bar{t}h \rightarrow t\bar{t}b\bar{b}$ mode (Drollinger), and the fact the the RS $\xi \neq 0$ scenarios predict at worst modest suppression

of this mode relative to the SM, it now seems that there is an excellent chance to see a $t\bar{t}h \rightarrow t\bar{t}b\bar{b}$ signal (and it should be for the same m_h as in the $gg \rightarrow h \rightarrow \gamma\gamma$ channel).

A quite interesting test of the model is possible.

The important point is that it should be possible to test for the presence of the anomalous part of the $gg \rightarrow h$ coupling that is so characteristic of the RS scenario if $\xi \neq 0$.

4. First, note that the anomalous $\gamma\gamma h$ coupling shows quite small deviations from its SM value and so we will neglect these deviations for now.

The result is that $B(h \rightarrow \gamma\gamma)$ and $B(h \rightarrow b\bar{b})$ are very nearly SM-like. All partial widths are scaled by g_{fVh}^2 but the ratios that define the B 's remain unchanged

(This assume we are not near the special 0 in g_{fVh}^2 . If we are then the gg decay mode of the h dominates and LHC discovery would be very hard.)

5. Second, note that if there were no anomalous $gg \rightarrow h$ coupling, then the $t\bar{t}h/ggh$ ratio would be the same as in the SM.

Both production rates would scale as g_{fVh}^2 .

6. So, the idea is to look at

$$R_{ttgg} \equiv \frac{\left[\frac{\sigma(t\bar{t}h \rightarrow t\bar{t}b\bar{b})}{\sigma(gg \rightarrow h \rightarrow \gamma\gamma)} \right]}{\left[\frac{\sigma(t\bar{t}h_{\text{SM}} \rightarrow t\bar{t}b\bar{b})}{\sigma(gg \rightarrow h_{\text{SM}} \rightarrow \gamma\gamma)} \right]} . \quad (15)$$

If $R_{ttgg} = 1$ then there is no reason to believe that Higgs-radion mixing is present.

If $R_{ttgg} \neq 1$, one could imagine a $\xi \neq 0$ RS interpretation.

7. In fact, R_{ttgg} deviates very substantially from 1 in general, to an extent

that would probably be measurable.

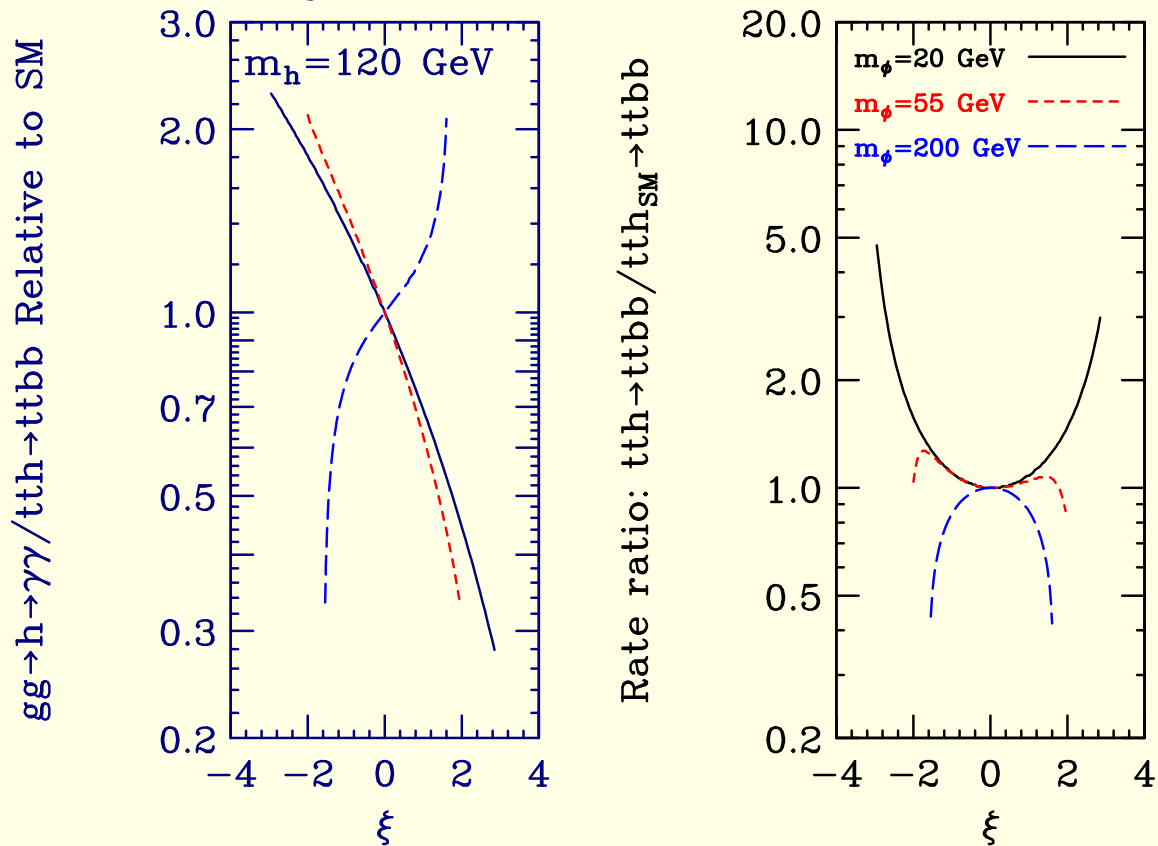


Figure 14: The ratio R_{ttgg} as a function of ξ for our standard m_ϕ values and $\Lambda_\phi = 5$ TeV. Also plotted (again) is the $t\bar{t}h \rightarrow t\bar{t}b\bar{b}$ rate relative to that for the h_{SM} , showing a good signal rate.

8. Given $R_{ttgg} \neq 1$, we would have evidence of an anomalous $gg \rightarrow h$ coupling contribution.

Combining with one of the independent rates, say $gg \rightarrow h \rightarrow \gamma\gamma$, we have two constraints on ξ and m_ϕ and could possibly solve for them.

9. If we were lucky enough to also see the ϕ , and the value of m_ϕ agreed with the above determination and the $gg \rightarrow \phi \rightarrow 4\ell$ agreed also, we would have pretty solid evidence for the RS Higgs-radion scenario with $\xi \neq 0$.
10. The LC would completely clinch the case by measuring g_{ZZh}^2 ($= g_{fVh}^2 \times$ SM value) and check that the other couplings are roughly rescaled by the same multiplicative factor.
And, of course, the LC might also see the ϕ , which would provide all kinds of independent checks.

- Determination of absolute couplings?

- If you can rely on the branching ratios being something close to SM-like, then any absolute cross section measured at the LHC can be converted to a coupling strength squared for the colliding partons to the Higgs.

This is not a completely certain game in the radion-Higgs scenario since g_{ggh}^2 is anomalously large. But, $B(h \rightarrow gg)$ still remains below about 10% implying no more than about a 10% error in this assumption.

- **Examples:**

$$\frac{\sigma(WW \rightarrow h \rightarrow F)}{B(h \rightarrow F)} \propto g_{WW h}^2 \quad (16)$$

where $F = WW^{(*)}, \tau^+\tau^-$ might be useful.

Same story for $t\bar{t}h$:

$$\frac{\sigma(t\bar{t}h \rightarrow t\bar{t}F)}{B(h \rightarrow F)} \propto g_{t\bar{t}h}^2 \quad (17)$$

for any F final state in which a signal can be seen.

In this way one would get several different determinations of $g_{fVh}^2 = (d + \gamma b)^2$.

Given a Λ_ϕ determination from KK information (so that $\gamma = v/\Lambda_\phi$ is known), this would really start to pin the ξ parameter down.

Of course, all the determinations of g_{fVh}^2 should agree with one another (even though you don't know $B(h \rightarrow gg)$ exactly).

If they don't, the radion-Higgs scenario would be unlikely.

Conclusions

- The mixing of the Higgs field with the radion field induces changes in the production and decay properties of the Higgs boson mass eigenstate.
- Such changes may weaken, or even invalidate, the expectations obtained in earlier studies for observability of the Higgs boson.
- For almost the entire region of the parameter phase space where the suppression of the Higgs signal yield causes the overall signal significance at the LHC to drop below 5σ , the radion eigenstate ϕ can be observed in the $gg \rightarrow \phi \rightarrow Z^0 Z^{0(*)} \rightarrow 4 \ell$ process instead.
- There is promise that it might be possible to extract evidence for the predicted anomalous component of the ggh coupling by finding

$$R_{ttgg} = \frac{\left(\frac{ttbb}{\gamma\gamma}\right)}{(\dots)_{SM}} \neq 1. \quad (18)$$

The value of R_{ttgg} and one of the ingredient rates (e.g. $gg \rightarrow h \rightarrow \gamma\gamma$) would fix ξ and m_ϕ to some accuracy (study needed) if Λ_ϕ were constrained by KK observation.

Of course, if the ϕ were also observed, thereby determining m_ϕ , a value of Λ_ϕ could be extracted independently of KK observations.

- If one temporarily assumes the radion-Higgs scenario, determinations of g_{WW}^2 and $g_{t\bar{t}h}^2$ from WW fusion and $t\bar{t}h$ production would be possible to about 10% based on the model input that $B(h \rightarrow gg) \leq 10\%$.

These determinations should agree (within errors) or the radion-Higgs scenario is not the correct one.

- An e^+e^- linear collider would effectively complement the LHC both for the Higgs observability, including the most difficult region at low m_ϕ and positive ξ values, and for the detection of the radion mixing effects, through the precision measurements of the Higgs particle couplings to various types of particle pairs.

As above, all such determinations should agree with one another (aside from the ggh and $\gamma\gamma h$ couplings which have anomalous contributions). If they don't, the radion-Higgs idea is not correct.

- We stress again that the Higgs-radion sector is not the only means for probing the Randall-Sundrum type of model.

The scenarios considered here will also yield the distinctive signature of KK graviton excitation production at the LHC.

This easily observed signal will serve as a warning to look for a possibly mixed Higgs-radion sector and help constrain the all-important Λ_ϕ parameter.